Available online at www.sciencedirect.com

ScienceDirect

Journal of Nuclear Materials 363–365 (2007) 751–758

journal of nuclear materials

www.elsevier.com/locate/jnucmat

Behaviors of impurity and hydrogen recycling on the HT-7 tokamak

Juan Huang *, Baonian Wan, Xianzu Gong, Zhenwei Wu, the HT-7 Team

Institute of Plasma Physics, Chinese Academy of Sciences, P.O. Box 1126, Hefei, Anhui 230031, PR China

---

Abstract

Behaviors of impurity and hydrogen recycling are investigated based on passive spectroscopy measurement on HT-7. During LHCD long pulse discharges, impurity and hydrogen recycling shows complicated aspects in different phases depending on wall properties. An uncontrollable density increase is observed, correlated with impurity concentrations, injected energy and local heat flux on the limiter. Under certain conditions, high impurity radiation and uncontrollable density can reduce LHCD efficiency and thus lead to discharge termination. To reduce impurity levels, RF wall conditioning was applied. After boronization, high hydrogen emission led to uncontrollable density rise. When the $H/(H+D)$ ratio was reduced to less than 25%, the electron density was easily controlled. The longest discharge up to 306 s with central electron temperature $T_e(0) \sim 1.0$ keV and central electron density $n_e(0) \sim 0.8 \times 10^{19}$ m^{-3} was achieved. The evolution of recycling behavior has been investigated during long pulse discharges in terms of $H/(H+D)$ ratio and the edge-recycling coefficient R.

PACS: 52.40.Hf; 52.25.Vy

Keywords: Boronization; Wall recycling

---

1. Introduction

The increase in discharge duration and plasma energy in future fusion devices will give rise to important plasma–material interaction effects that will critically influence the plasma performance. Impurity and wall recycling control are key issues for achievement of steady-state operation. The two essential impurity production processes occurring at the first wall are physical and chemical sputtering [1–3]. Many experiments on impurity behaviors and transport have been performed in tokamaks, and a well-known database for these various processes is described in [4–9]. Karney and Fisch [10] have observed that a high impurity concentration can reduce the LHCD efficiency and thus limit long pulse operation. Under certain conditions of lower hybrid wave driven current, I_{rf}, and electron density, n_e, wall conditioning can enhance the current drive efficiency, thus reducing the required LHCD power [11]. This lower LHCD power required for achieving the full potential plasma performance also

---

* Corresponding author. Fax: +86 055 559 1310.
E-mail address: janejoy@ipp.ac.cn (J. Huang).

0022-3115/$ - see front matter © 2007 Elsevier B.V. All rights reserved.
doi:10.1016/j.jnucmat.2007.01.060

reduces plasma wall interactions. The main issues are controlling the generation of plasma impurities and the recycling hydrogenic fluxes. In addition, uncontrollable density can also lead to discharge terminations due to a large amount of particles from edge recycling in a 1-min discharge of JET [12]. Increase of plasma density during long plasma operation was observed in Tore Supra [13]. Therefore, there have been many studies of the particle recycling behavior [14,15], which is also very critical to future tokamaks.

As a superconducting tokamak, the main efforts of the HT-7 program are to develop the physics and technologies for steady-state operation. Impurity and recycling control are very important in obtaining reproducible non-inductive current drive discharges. One of the main purposes of the 2005 experimental campaign was to explore characteristics of HT-7 long pulse operation. The longest discharge achieved (duration of 306 s) had a central electron temperature $T_e(0)$ of $\sim$1.0 keV and a central electron density $n_e(0)$ of $\sim 0.8 \times 10^{19}\ \mathrm{m}^{-3}$. Wall coating was achieved by means of ICRF boronization using carborane ($C_2B_{10}H_{12}$) powder as the boronization material. This technique has been demonstrated to be very effective for impurity reduction of the plasma discharge, which has been routinely used in the HT-7 tokamak during the past few years [16,17]. However the large amount of hydrogen contained in the fresh boron film, due to a high content of hydrogen in the carborane, caused a serious hydrogen emission problem. Understanding the control of the recycling behavior is important for further progress in long pulse discharges and is discussed in this paper. Recycling is examined using the $H/(H+D)$ ratio inferred from the $D_\alpha(H_\alpha)$ spectrum and the recycling coefficient R obtained using the particle equilibrium equation [18].

In this paper, following the introduction of Section 1, the experimental configuration and a description of relevant diagnostics is given in Section 2. Section 3 describes impurity behavior in LHCD discharges; uncontrollable density increase in long pulse discharges, correlated with the impurity influx is mainly attributed to parts of the first wall. The reduction of impurity, as well as plasma performance improvement by ICRF boronization is shown in Section 4. The evolution of hydrogen recycling behavior after boronization in terms of the $H/(H+D)$ ratio and the edge-recycling coefficient R is discussed in Section 5. Finally, Section 6 is a short summary.

2. Experimental configuration and diagnostic description

HT-7 is a medium sized tokamak with active water-cooled up–down symmetrical toroidal limiters and belt limiters located at the high field side. A new form of doped graphite with a SiC gradient coating is chosen as a plasma facing material to reduce chemical erosion and accommodate the requirements of long pulse plasma. The main machine parameters are major radius $R = 1.22$ m, minor radius $a = 0.27$ m, plasma current $I_p = 50$–250 kA, line averaged density $\bar{n}_e = 0.5\text{–}6.5 \times 10^{19}\ \mathrm{m}^{-3}$, central electron temperature $T_e(0) = 0.3$–3.0 keV, toroidal magnetic field $B_T = 1.0$–2.5 T. The working gas is deuterium, with the central line averaged electron density regulated by feedback control of gas valve deuterium injection, measured by a far infrared interferometer. LHCD at a frequency of 2.45 GHz is used both for sustaining the plasma current and current density profile control. Ion Bernstein Wave (IBW) heating with a frequency of 24.5–30 MHz for controlling the electron pressure profile can be integrated into LHCD plasmas and improve the localization of LHCD [19,20]. An active research program in steady-state plasma operation has been followed in the last few years.

Impurity emissions were measured by passive spectroscopy in the visible and ultraviolet range [18]. Two Optical Multi-channel Analysis (OMA) systems were used. One is equipped with an Acton Research Spectrometer (SP-300i) as a survey spectrometer to measure the impurity spectral lines in a wide spectral range. The other system is equipped with a high-resolution spectrometer (SP-750) to measure the $D_\alpha(H_\alpha)$ spectral line shape. The sum of the D_α and H_α emission was measured by two interference filter scopes with photodiode arrays, which cover the whole poloidal cross-section of the plasma. For fast signals described in this paper, the temporal behavior of the light impurity emissions (CIII at 464.7 nm, OII at 441.5 nm) was measured by two monochromators coupled by optical fiber bundles, with lines of sight passing through the plasma center.

3. Impurity behavior in long pulse operation

Impurity influxes of carbon and oxygen in HT-7 played a dominant role during long pulse operation, showing different behaviors and time evolution. Oxygen is assumed to originate from water desorption in the inner vessel, from areas far from plasma wetted zones which are not baked by wall heating. Carbon mainly comes from erosion and sputtering of PFC. Passive spectroscopy in the visible and ultraviolet range in various operation conditions is used to assess these behaviors. In HT-7, the available LHCD allows a decrease of the loop voltage close to zero (implying fully non-inductive current) only for lower central electron density ~ 0.5–$1.0 \times 10^{19}\ \mathrm{m}^{-3}$ and plasma current about 50–100 kA. In long pulse discharges with lower density and plasma current, high carbon and oxygen impurity concentrations follow the increase in injected energy and plasma duration, which leads to increases in the global recycling to and above unity, although the radiated power is low at relatively lower LHCD power (100–200 kW) in this case. The waveforms of an over 2 min shot are plotted in Fig. 1. The discharge was stable for 120 s. At the end of the discharge, the uncontrollable density rise was strongly correlated with the oxygen and carbon influx, following the rapid increase of the limiter surface temperature and the discharge was terminated. IR images from the high heat flux region on the belt limiter at High Field Side (HFS), show that the highest temperature of the limiter was even more than 800 °C [21].

An increase in density will lead to a lowering of current driven efficiency and then to an increase in magnetic flux consumption incompatible with constant plasma current. To maintain a constant plasma current and obtain full non-inductive current in a long pulse discharge, LHCD power has to be increased during the density rise [13]. However, this much higher LHCD power causes a larger heat flux loading on the limiter surface, leading to impurity production and reduced current drive efficiency. In order to enhance heat exhaust capability, since 2004, a new active water cooling up–down toroidal limiter has been installed, the limiter area is enlarged up to $1.88\ \mathrm{m}^2$. Copper alloy heat sink instead of stainless steel were applied to improve thermal conductively [22]. The experimental results show that the LHCD power needed to sustain the plasma current increases with the product $I_\mathrm{p} * n_\mathrm{e}$. The relation of t_n versus $I_\mathrm{p} * n_\mathrm{e}$ is shown in Fig. 2, where t_n is the time at which the uncontrollable density increase begins and $I_\mathrm{p} * n_\mathrm{e}$ is proportional to the radiated power. The time for uncontrollable density is directly correlated with the injected LHCD energy. t_n decreases with increasing $I_\mathrm{p} * n_\mathrm{e}$ as well as injected energy.

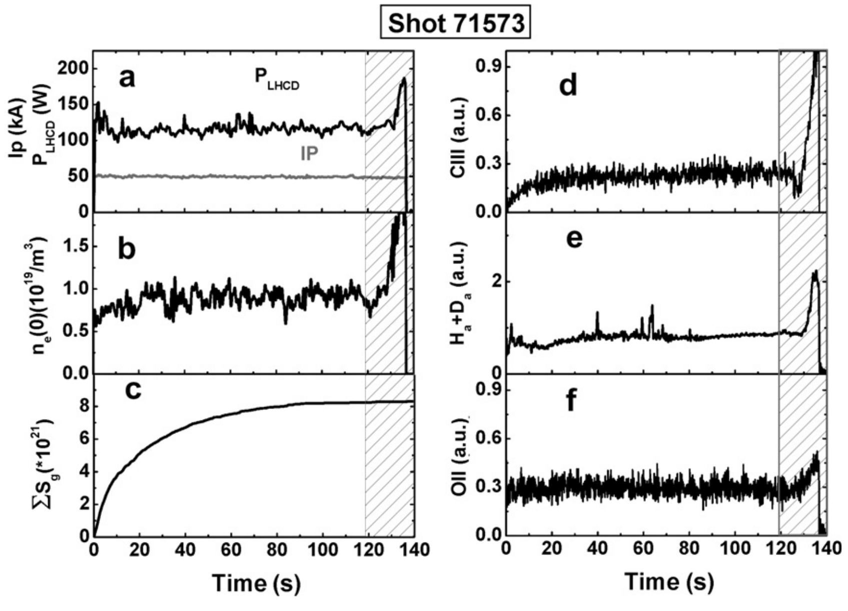

Fig. 1. Uncontrollable density with high impurity radiation and recycling in a 2 min long pulse discharge (shot 71 573). (a) Plasma current, P_{LHCD}, (b) central line averaged plasma density, (c) total amount of gas supply, (d) carbon radiation, (e) Ha emission from the limiter surface, and (f) oxygen radiation.

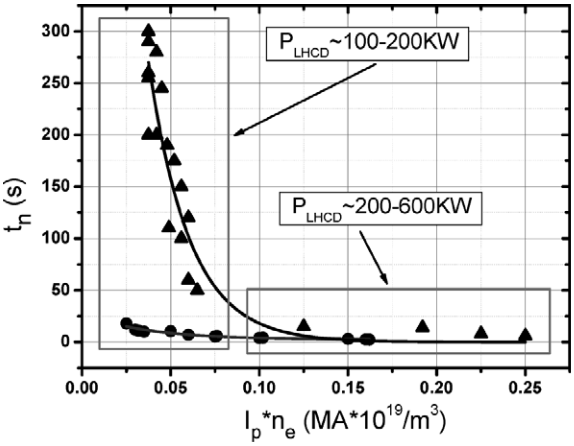

Fig. 2. The relation between the product of $I_p * n_e$ (i.e. the radiated power) and t_n. Triangles are chosen from the 2004 and 2005 experimental campaigns, when the toroidal up–down limiter was applied for enhanced heat exhaust capability. Dots are from the 2003 experimental campaigns.

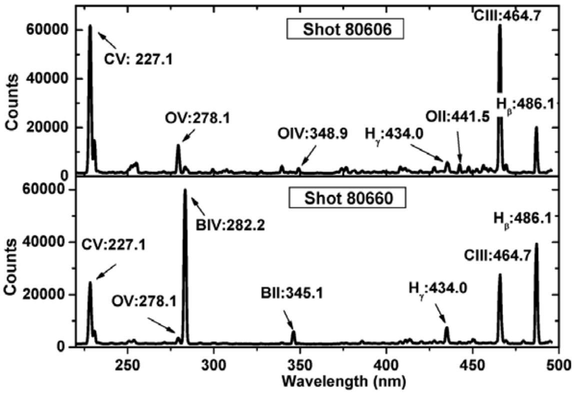

Fig. 3. Comparison of impurity spectral lines for two typical Ohmic discharges, shot 80 606 (before boronization) and 80 660 (after boronization), measured by the SP-300i OMA, where there are nearly the same central line averaged electron density $\bar{n}_e = 1.5 \times 10^{19}\ \mathrm{m}^{-3}$, $I_p = 125$ kA, and $B_T = 1.8$ T.

4. Impurity reduction by ICRF boronization

For long pulse discharges, the impurity control is the most serious constraint. It can be partially solved by special magnetic configuration control, in parallel with the development of high performance plasma facing components and wall conditioning [23,24], as in HT-7. ICRF wall-conditioning techniques, especially ICRF boronization, have been routinely used to reduce impurity levels in the HT-7 tokamak. Plasma impurity spectral lines for two typical ohmic discharges before and after ICRF boronization are presented in Fig. 3, measured by the SP-300i. These two shots had nearly the same central line averaged electron density $\bar{n}_e = 1.5 \times 10^{19}\ \mathrm{m}^{-3}$ and constant $I_p = 120$ kA, $B_T = 2.0$ T. The data clearly indicate that the spectral line intensities of carbon and oxygen impurity were reduced to a low level following boronization. Also, soft X-ray measurements demonstrated an order of magnitude reduction of radiation from metallic impurities. Clearly, this is due to the shielding effect of boronization induced coatings of metallic surfaces. Consistent with XUV measurements, the total radiated power decreased sharply to the level of 20% of the ohmic power, while it is usually 50–90% without boronization. Z_{eff} dropped dramatically to a value close to 1.8. This indicates that significantly reduced impurity levels characterize plasma performance improvements. These characteristics of the boundary plasma are favorable for good confinement, improving both energy and particle confinement times [22]. Evaluations of impurities emission as function of discharge number before and after boronization are shown in Fig. 4. The oxygen and carbon was further reduced with RF-boronization. Under certain lower hybrid wave driven current, I_{CD}, and electron density, n_e, conditions, wall conditioning can enhance the current drive efficiency, thus reducing the requirement on LHCD power. This lower LHCD power injection can reduce plasma wall interactions and prevent an earlier occurrence of the uncontrollable density rise and extend the discharge duration, allowing achievement of the full potential plasma performance.

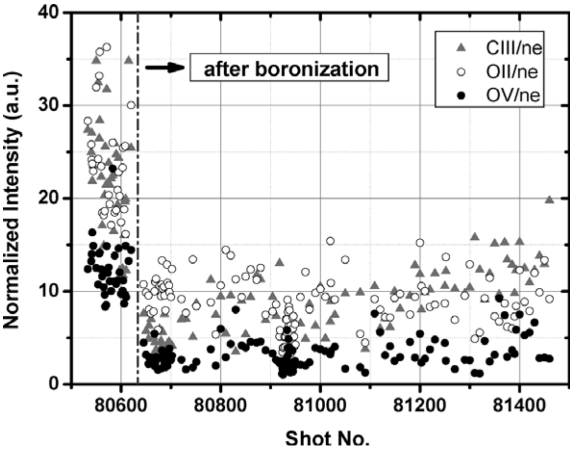

Fig. 4. Evolution of impurity emission as function of discharge number before and after boronization.

5. Hydrogen recycling

However the large amount of hydrogen contained in the fresh boron film after boronization, caused a serious hydrogen recycling problem. Understanding control of the recycling behavior is important for further progress in long pulse discharges. Hydrogen recycling is examined using the $H/(H+D)$ ratio inferred from the $D_\alpha(H_\alpha)$ spectrum and the recycling coefficient R. Fig. 5 shows $H/(H+D)$ ratio in the long pulse mode as a function of discharge number after boronization. The hydrogen recycling behavior after boronization can be divided into three different phases labeled in Fig. 5, discussed in the following text.

During the phase of uncontrollable density, Fig. 5, labeled (1), the measurements of $D_\alpha(H_\alpha)$ line shapes show a very high $H/(H+D)$ ratio ($\geqslant$70%) and even 90% at the first few shots. The hydrogen fraction is high due to the fresh a-C/B:H film that contains a large amount of co-deposited hydrogen. The high recycling and uncontrollable density in Phase (1) is different from the behavior reported in previous ICRF boronization [16] in which the density could be easily controlled. A major difference is that in the present work extensive further helium discharge cleaning with high power and long duration was not applied [18]. This was done in order to obtain sufficient film thickness suitable for long pulse discharges.

During the phase of transition to the controllable density, Fig. 5, labeled (2), the ratio was reduced to 25–65%. Electron density could be controlled for ohmic discharges. But, when LHCD was applied, edge hydrogen recycling still limited the discharge duration. Fig. 6 shows the waveforms of a shot in this phase. The line intensities of carbon and oxygen impurities were reduced to very low levels, Fig. 6(d), with very little increase due to the increased plasma density. Up to 2.5 s the recycling coefficient R was less than 1, Fig. 6(f), which indicated the plasma density was controllable by the feedback control of gas injection. The recycling coefficient R was above unity after 2.5 s, the density had a rapid increase because of increasing hydrogen from the film, Fig. 6(e), and the gas puff was stopped, Fig. 6(c). In this case the $H/(H+D)$ ratio was still high, up to 60%, and hydrogen recycling was dominant. In this phase the LHCD efficiency was not high enough to sustain the plasma at a certain plasma current and electron density for a long duration. Thus larger LHCD power should be injected, but higher LHCD power injection will cause an increase in the heat load on the surfaces of the wall and limiters and accelerate the release of hydrogen and deuterium. According to the analysis described above the released particles were mainly composed of hydrogen from the film. The high release rate led to high hydrogen and deuterium recycling which caused the plasma density to increase rapidly and terminated the discharge.

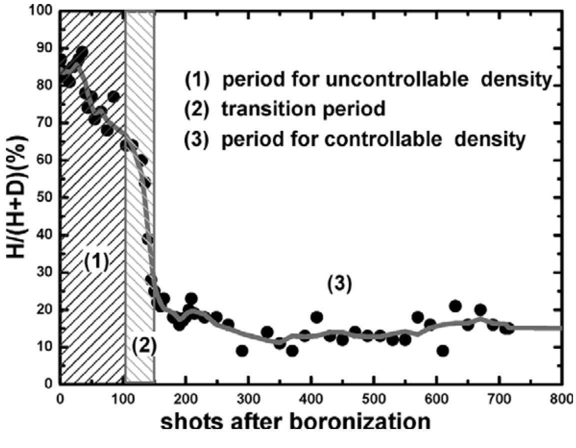

Fig. 5. $H/(H+D)$ ratio in the long pulse mode as a function of discharge number after boronization, Phases 1, 2 and 3 are discussed in the text.

To obtain long pulse discharges, reducing the high edge recycling is most important both for effective LHCD efficiency and density controllability. After about 150 shots with total cumulative duration 800 s, the $H/(H+D)$ was reduced to less than 25%, Fig. 5, Phase (3). The density control was easily achieved, because hydrogen was continually removed from the fresh film by discharges and partly replaced by deuterium. Fig. 7 shows the typical discharge waveforms of a shot in this period at about 300 shots after boronization. It indicates that LHCD efficiency was high enough to sustain the long pulse discharge. The duration of this discharge was pre-set up to 125 s with $P_{\mathrm{LHCD}} =$ 140 kW, Fig. 7(a). The $H/(H+D)$ ratio was about 15%, Fig. 7(d). The central line averaged electron density, Fig. 7(b), was kept almost constant by feedback controlled fueling, Fig. 7(c). In Fig. 7(h), R increased and reached a stable level at about 40 s, so the electron density was under good control. The emission of H_α and D_α, Fig. 7(f), was also kept stable and low which means that the level of edge hydrogen recycling was stable and low. In Fig. 7(e) the emission of carbon from limiter

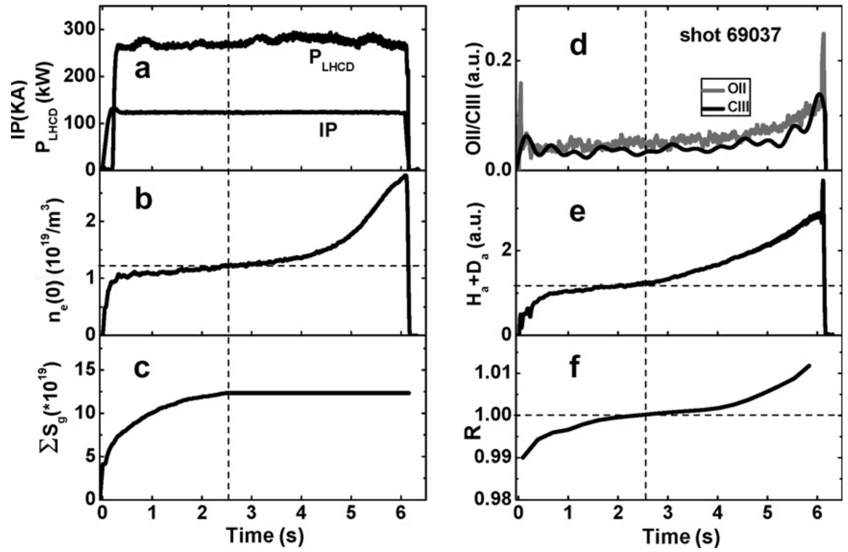

Fig. 6. The temporal time evolution for the typical LHCD discharge (shot 69037 the center electron temperature $T_e(0) = 1.5$ keV, the averaged heat load on the limiter ~0.4 MW/m^2) during the phase of transition to controllable density. (a) Plasma current, and P_{LHCD}, (b) central line averaged plasma density, (c) total amount of gas supply, (d) carbon and oxygen radiation, (e) $H_\alpha + D_\alpha$ emission from the limiter surface, and (f) the recycling coefficient R.

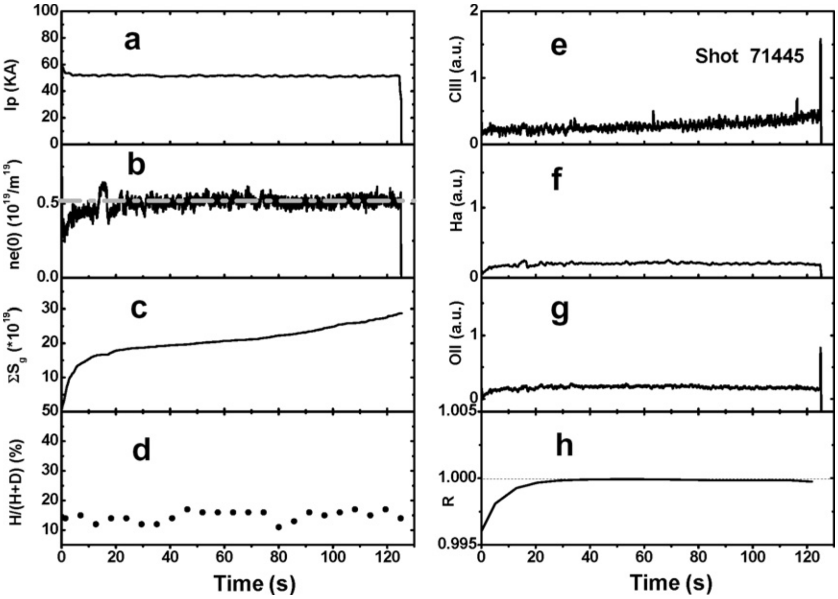

Fig. 7. The waveforms of shot 71445 from the phase of controllable density. (a) Plasma current, $I_p \sim 50$ kA, (b) central line averaged plasma density, (c) total amount of gas supply, (d) the $H/(H+D)$ ratio, carbon (e), H_α+D_α (f), and oxygen (g) emission from the limiter surface, and (h) the recycling coefficient R.

surfaces was very low but had a small increase while in Fig. 7(g) that of oxygen was kept constant. This may be because the stronger chemical bonding of oxygen than carbon to boron might trap the oxygen ions and atoms leaving the plasma and reduce oxygen re-emission [25]. This shows that after the accumulation of the total cumulative effective discharge duration of about 10^4 s, the boron film can still

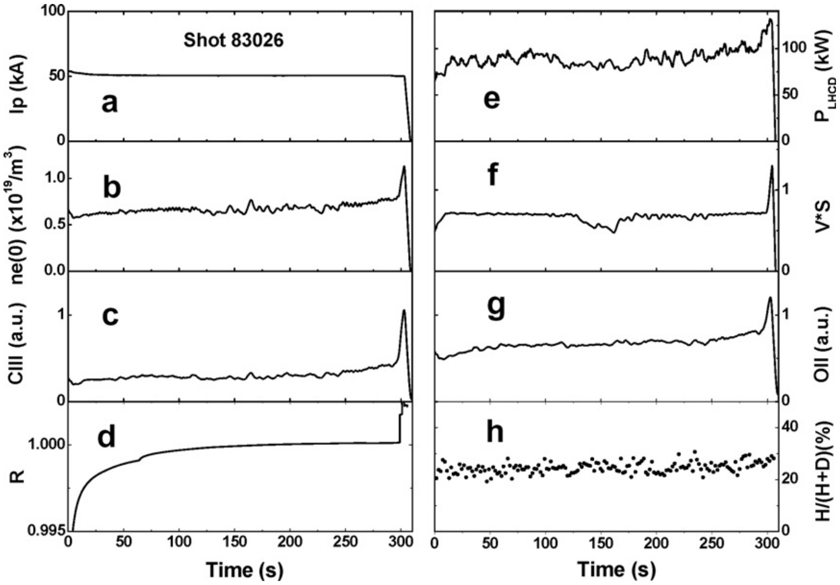

Fig. 8. The longest pulse discharge (shot 83026) with a duration of 306 s with $T_e(0) \sim 1.0$ keV. (a) Plasma current, $I_p \sim 50$ kA, (b) central line averaged plasma density, $n_e(0) \sim 0.8 \times 10^{19}\ \mathrm{m}^{-3}$, (c) carbon radiation, (d) recycling coefficient R, (e) injected power of LHCD, (f) magnetic flux, (g) oxygen radiation, and (h) ratio of $H/(H + D)$.

reduce the oxygen influx and maintain long duration discharges.

The main characteristics of this period are that (1) both the level of impurities and the edge recycling are very low, (2) the target plasma has good performance and (3) the LHCD efficiency is high. With these features, as well as necessary technical improvements and optimized plasma control in the HT-7 tokamak [22], the longest pulse discharges with a duration of 306 s, $T_e(0) \sim 1.0$ keV and central electron density $n_e(0) \sim 0.8 \times 10^{19}\ \mathrm{m}^{-3}$ were achieved, shown in Fig. 8. The main problem for extending long pulse discharges even further is not edge recycling but how to control the plasma position. Improper positioning often leads to excessive temperatures in a local part of the limiter [21], which then terminates the discharge.

6. Summary

An uncontrollable increase in plasma density during long pulse operation is observed in the HT-7 superconducting tokamak due to much higher injected power and higher radiated energy from the plasma. A fast rise in density leads to a decrease of LHCD efficiency and in turn to an increase in the magnetic flux consumption, which limits the plasma discharge duration. This behavior is correlated with an increase in impurity radiation. In order to control density and reduce impurities, ICRF boronization is applied, allowing the achievement of reproducible discharges suitable for steady-state operation. The fresh a-C/B:H film can reduce the impurity radiation to very low levels, especially oxygen, but the recycling coefficient can exceed unity due to the large amount of hydrogen absorbed in the coatings, leading to an uncontrollable density rise and discharge termination. Hydrogen recycling behavior was studied in the HT-7 tokamak, which exhibits different features during long pulse operation after ICRF boronization, relative to unboronized conditions. After many plasma discharges the ratio $H/(H + D)$ is reduced to 25–65%, electron density can be controlled for ohmic discharges, but the LHCD efficiency is very low. A high LHCD power is therefore required at this point to sustain long pulse discharges. When the ratio is reduced to less than 25%, the hydrogen recycling becomes stable and the electron density is easily controlled. As a result, the longest discharge with $T_e(0) \sim 1.0$ keV, $n_e(0) \sim 0.8 \times 10^{19}\ \mathrm{m}^{-3}$ (almost steady-state conditions) has been achieved with duration of 306 s. In the future, efforts are continuing to investigate recycling and particle exhaust technology and physics under steady-state condition.

Acknowledgement

This work has been supported partially by the JSPS-CAS Core – University Program in the field of 'Plasma and Nuclear Fusion'.

References

[1] P.C. Stangeby, G.M. McCracken, Nucl. Fusion 30 (1990) 1225.
[2] W. Eckstein, J. Bohdansky, J. Roth, Nucl. Fusion 1 (Suppl.) (1991) 51.
[3] J. Roth, E. Vietzke, A.A. Haasz, Nucl. Fusion 1 (Suppl.) (1991) 63.
[4] G. Fussman et al., J. Nucl. Mater. 145–147 (1987) 96.
[5] P.C. Stangeby, D. Elder, Nucl. Fusion 35 (1995) 1391.
[6] G.R. Smith et al., J. Nucl. Mater. 220–222 (1994) 1024.
[7] A. Taroni et al., Proceedings of 22nd European Conference on Controlled Fusion and Plasma Physics, vol. 19C, Part IV, European Physical Society, Geneva, Bournemouth, 1995, p. 297.
[8] A. Kallenbach, R. Neu, W. Poschenrieder, Nucl. Fusion 34 (1994) 1557.
[9] M.R. Wade et al., Proceedings of 23rd European Conference on Controlled Fusion and Plasma Physics, vol. 20C, Part I, European Physical Society, Geneva, Kiev, 1996, p. 283.
[10] C.F. Karney, N. Fisch, Phys. Fluids 28 (1985) 116.
[11] F. Leuterer et al., Nucl. Fusion 31 (1991) 2315.
[12] M. Brusati et al., Controlled fusion and plasma physics, Proceedings of 19th Eur. Conference, Innsbruck, 1992, vol. 16C, Part I, European Physical Society, Geneva, 1992, p. 307.
[13] C. Grisolia, Tore Supra Team, J. Nucl. Mater. 266–269 (1999) 146.
[14] V.M. Chicherov et al., J. Nucl. Mater. 145–147 (1987) 117.
[15] G.L. Jackson et al., J. Nucl. Mater. 196–198 (1992) 236.
[16] J.G. Li, Y.P. Zhao, et al., Nucl. Fusion 39 (1999) 973.
[17] J.K. Xie, Y.P. Zhao, J.G. Li, et al., J. Nucl. Mater. 290–293 (2001) 1155.
[18] J. Huang et al., Nucl. Fusion 46 (2006) 62.
[19] B.N. Wan et al., Nucl. Fusion 44 (2004) 400.
[20] B.N. Wan et al., Phys. Plasmas 11 (2004) 2543.
[21] H. Lin, et al., J. Nucl. Mater., these Proceedings, doi:10.1016/j.jnucmat.2007.01.115.
[22] X. Gong, et al., J. Nucl. Mater., these Proceedings.
[23] J. Winter et al., J. Nucl. Mater. 162–164 (1989) 713.
[24] S. Veprek et al., J. Nucl. Mater. 162–164 (1989) 724.
[25] F. Waelbroeck et al., Plasma Phys. Controlled Fusion 31 (1989) 185.